



Original Research Article

A DFT and Molecular Dynamic (MD) Simulation on the Adsorption of Vidarabine as a Potential Inhibitor on the Al Metal surface

Fater Iorhuna ¹ * , Abdullahi Muhammad Ayuba ¹ , Thomas Aondofa Nyijime ² , Muhammad Shuaibu ¹

¹Department of Pure and Industrial Chemistry, Faculty of Physical Sciences, Bayero University, Kano, Nigeria

²Department of Chemistry, College of Physical Sciences, Federal University of Agriculture, Makurdi, Nigeria

ARTICLE INFO

Article history

Submitted: 02 July 2023

Revised: 17 August 2023

Accepted: 27 August 2023

Available online: 30 August 2023

Manuscript ID: [AJCA-2308-1390](https://doi.org/10.48309/AJCA.2308-1390)

Checked for Plagiarism: **Yes**

DOI: [10.48309/AJCA.2023.409740.1390](https://doi.org/10.48309/AJCA.2023.409740.1390)

KEYWORDS

Physiosorption

DFT

MD

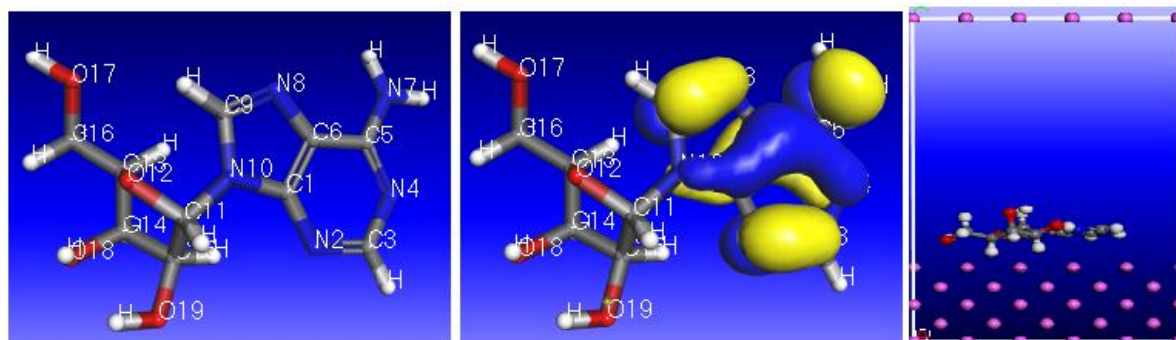
Vidarabine

Aluminium

ABSTRACT

In this study, DFT and molecular dynamic (MD) modeling were used to conduct a theoretical investigation of the potential inhibition of corrosion on Al by vidarabine. The local, global, and Fukui functions were used to calculate the molecule's reactivity. It is hypothesized that vidarabine will display physisorption with Al surface based on the predicted adsorption energy of the system and the binding energies obtained (58.923, -58.923 Kcal/mol). The negative value of the EHOMO, which is -5.050 eV, predicts the mechanism of vidarabine on the surface of Al to be physisorption. The molecular dynamics and the quantum properties suggest that the molecule vidarabine can operate as a potent corrosion inhibitor.

GRAPHICAL ABSTRACT



* Corresponding author: Iorhuna, Fater

✉ E-mail: uyerfater22@gmail.com

© 2023 by SPC (Sami Publishing Company)

Introduction

Corrosion of metals is a natural phenomenon arising from their metallic state. The most common reason for metal failures nowadays, surpassing other failure modes like fatigue, creep, impact, and others, is corrosion, which is thus unavoidable for metals and alloys [1]. Loss of production due to failure, high maintenance costs, adherence to consumer and environmental regulations, loss of product quality due to contamination from corrosion of the materials, high fuel and energy costs as a result of leakage from corroded pipes, additional working capital, and more extensive inventories are just a few of the areas where the cost of corrosion is overwhelming [2,3]. Corrosion can only be reduced. The engineering and construction industries are currently being disrupted by this ugly phenomenon [5]. Researchers have developed various corrosion prevention approaches to combat the threat of this corrosive impact. Altering the component or altering the environment are the two guiding ideas of the approaches that are now accessible. The component can be altered by making design changes, which are particularly effective when the corrosion is influenced by fluid flow properties (erosion-corrosion, cavitation), the presence or absence of gaseous phases (cavitation, pitting), contacts between dissimilar metals (galvanic corrosion), and solution stagnation (crevice corrosion) [1,2].

Before now, the use of inorganic inhibitors such as lead and painting of metals was in place for the inhibition of metals; however, due to the toxicity of some of these inorganic inhibitors, scientists began to search for alternative inhibitors. The use of organic compounds containing polar functions N, S, and O atoms and conjugated double bonds or aromatic rings in their molecular structure has become a fertile environment for searching for suitable inhibitors with adsorption centers [4].

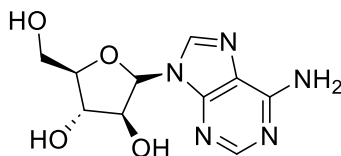
The theoretical method using DFT and MD simulation is quick and significant in the study of corrosion because it gives researchers a relatively quick way to examine the structure and behavior of corrosion inhibitors in contrast to other methods like weight loss, potentiodynamics, and galvanic method, which require time and resources [1,3,6,7]. Applying theoretical parameters enables describing inhibitors' chemical structures and offers a theory for how they interact with metal surfaces [2]. Molecular dynamic simulation can determine the interaction and adsorption energy between the inhibitor molecule and metal surfaces [1,5]. Recent theoretical investigations that modeled compounds' electrical, structural, and molecular characteristics identified as prospective corrosion inhibitors using computational methods found that these compounds are either inorganic, organic, or condensed matter [6-8]. Therefore, the theoretical method can be used in any form to depict the reactivity of any compound.

In this work, theoretical DFT and simulation (on the Al (110) surface) method were used to explore the corrosion inhibition potential of vidarabine (VDB) (2-(6-Amino-purin-9-yl)-5-hydroxymethyl-tetrahydrofuran-3,4-diol) compound. The molecule was chosen based on the presence of glycosides with the idea that, since glycosylated compounds are a proven platform for creating many existing front-line drugs, they may also be able to treat pure metals produced over time [9]. Al (110)'s aluminum crystal surface was selected because of its closed pack and density coverage [10].

The research of vidarabine (VDB) was aimed at determining the modes of adsorption on the Al surface, their adsorptive ability and the active sites of the molecule using Molecular Dynamic simulation. Considering properties such as binding energy, bond length and quantum chemical parameters such as energy of the highest occupied molecular orbital (E_{HOMO}), the

energy of the lowest unoccupied molecular orbital (E_{LUMO}), energy gap (ΔE), total energy (E), electron affinity (A), ionization potential (I), global hardness (η), global softness (S), Second

Fukui function and Fukui functions $f(r)$, at the lower possible energy with moderate temperature.



Scheme 1. Molecular structure of vidarabine

Computational Methods

Sketching and Geometric Optimization of the Molecules

Chem-Draw CambridgeSoft Ultra 7.0.3 was used to draw diagrams of the examined compound; to get a stable configuration, the molecular structure needs to be adjusted after construction. In order to achieve a stable state for the structure's energy or a state where the forces acting on the atoms are zero, the coordinates of the atoms are modified during this process. When the system is in equilibrium, it is predicted that the geometry corresponding to this structure would closely lower the system's actual physical structure [6–8]. To optimize the compound, the DMol³ optimization model, a function of BIOVIA Materials Studio 8.0 (Accelrys, Inc.), was used to lower the torsional and conformational energies of the molecules. Before the optimization, the compound was imported into Materials Studio from ChemDraw. The optimization used the following variables: DFT-D's restricted spin polarization DNP+ base. In the water solvent as B3LYP was selected as the local density functional [11–13].

Quantum Chemical Parameters Calculations

Per Koopman's theory, Equations (2) and (3), respectively, relate the energy of the border molecular orbital, the energy of the highest occupied molecular orbital (EHOMO), and the

energy of the lowest unoccupied molecular orbital (ELUMO) [14–17].

$$IE = -EHOMO \quad (1)$$

$$EA = -ELUMO \quad (2)$$

According to Pearson, the global hardness (η) value is approximated as shown in Equation (3). Equation 4 demonstrates that the system's global softness (S) is the opposite of the global hardness. While Equations 5 and 6 derive the global electrophilicity index and nucleophilicity, respectively [7,9].

$$\eta = \frac{IE - EA}{2} \quad (3)$$

$$S = \frac{1}{\eta} \quad (4)$$

$$\omega = \frac{\chi^2}{2\eta} \quad (5)$$

$$\varepsilon = \frac{1}{\omega} \quad (6)$$

Using the relationship provided in Equation 7, the energy gap of the molecules is computed. The energy gap is a factor that determines both the stability and reactivity of an inhibitor molecular structure.

$$\Delta Eg = ELUMO - EHOMO \quad (7)$$

Hence aluminum has a predicted electronegativity value of ($\chi_{Al}=5.6\text{eV}$) and a global hardness of 0 eV. Half-electron transfer (ΔN) in Equation 8 was computed, which shows the proportion of electrons transported from the

inhibitor to the surface of the metal. An indicator of the type of electron transfer between the inhibitor molecule and the metal surface.

$$\Delta N = \frac{\chi_{Fe} - \chi_{Inh.}}{2(\eta_{Fe} + \eta_{Inh.})} \quad (8)$$

Back donation is determined with the help of Equation (9)

$$\Delta E_{bd} = (\mu^+ - \mu^-)^2 / 4 \eta = \frac{-\eta}{4} \quad (9)$$

$$\chi = \text{Absolute electronegativity (eV)} \quad \chi = \frac{I+A}{2} = \frac{-1}{2}(E_{HOMO} - E_{LUMO}) \quad (10)$$

ω^- : electron donating power (eV)

$$\omega^- = \frac{(3IE+AE)^2}{16(IE-AE)} \quad (11)$$

ω^+ : electron accepting power (eV)

$$\omega^+ = \frac{(IE+3AE)^2}{16(IE-AE)} \quad (12)$$

The donating and acceptance of the molecule and the metal were described using the second-order Fukui function (f^2), also known as the dual descriptor $f(k)$ [2,5,31]. The distinction between the electrophilic and nucleophilic Fukui functions, as seen in Equation (15), is the second Fukui function (f^2) [14] where site $f(k)^+$ favors a nucleophilic attack when $f^2(r)$ is greater than zero, as opposed to an electrophilic assault when $f^2(r)$ is less than zero. This demonstrates that $f^2(r)$ is a selectivity index for nucleophilic or electrophilic assaults [14,19,20].

$$f(k)^+ \quad (\text{for nucleophilic attack}) \\ = qk(N+1) - qk(N) \quad (13)$$

$$f(k)^- \quad (\text{for electrophilic attack}) \\ = qk(N) - qk(N-1) \quad (14)$$

$$f(r) = f^+ \cdot f^- = f^2 \quad (\text{Fukui function}) \quad (15)$$

Molecular Dynamics Simulation

A simulation box measuring 17 x 12 x 28 with a periodic boundary condition was used to conduct a computational simulation to mimic the reality of the reaction between the molecule and the surface. To separate Al along the (110) plane, a fractional depth of 3.0 was utilized. The lower layers' form was constrained prior to iron surface optimization. Then, the Al surface was expanded into a 10 x 10 supercell [1,4,19] to reduce edge effects. Setting the temperature to quench the molecule on the surface at 350 K [1-2, 21]. With a time step of 1 fs and a simulation runtime of 5 ps, the temperature was established using the NVE (microcanonical) ensemble. The system was set up to quench every 250 steps on both surfaces to get statistical data for the energies on the surface of Al. Forcife-specific models and surface designs were used to create various interactions. The binding energy between the inhibitors and the metal surfaces is calculated using Equation 16 [22,31-34].

$$\text{Binding Energy} = E_{total} - (E_{inhibitor} + E_{Fe \text{ surface}}) \quad (16)$$

$$E_{adsorption} = -E_{binding} \quad (17)$$

Result and Discussion

Molecular Dynamic Simulation

The close contacts between the inhibitor and the aluminum surface were evaluated using the Forcife model in the BOVIA Material Studio (Accelrys, Inc.), where each step was quenched at 350 K [1]. Using the parameters of interaction such as binding energy, surface energy, total kinetic energy and adsorption energies, the nature of the interaction between the molecule and the surface was calculated with the aid of Equation (16) and the result was presented as shown in Table 1. The result depicts that the compound exhibits low binding and negative adsorption energy.

Ayuba and Umar reported that a more negative value of adsorption energy of the inhibitor-metal surface interaction, the better the adsorption of

the inhibitor onto the metal surface, the better the adsorption of the inhibitor onto the metal surface and, subsequently, the higher the inhibition. E_{binding} is equivalent to $-E_{\text{adsorption}}$ as presented in Equation (17). This indicates that the molecule VDB had mild adsorption on the aluminum surface; hence the binding energy exhibited by the interaction is -58 kJmol^{-1} [2, 22, 25]. This is also per Belghiti *et al.*, Nyijime *et al.*,

and Bello *et al.*, in their various research, stated that chemical adsorption would occur on the metal surface if the binding energy is $>100 \text{ kcalmol}^{-1}$ [19,20,31]. Thus, it is confirmed from the Molecular Dynamic simulation result in Table 1 that the binding energy is just $58.923 \text{ kcalmol}^{-1}$, less than 100 kcalmol^{-1} . This implies that the aluminum and vidarabine (Al-VDB) interaction was physical.

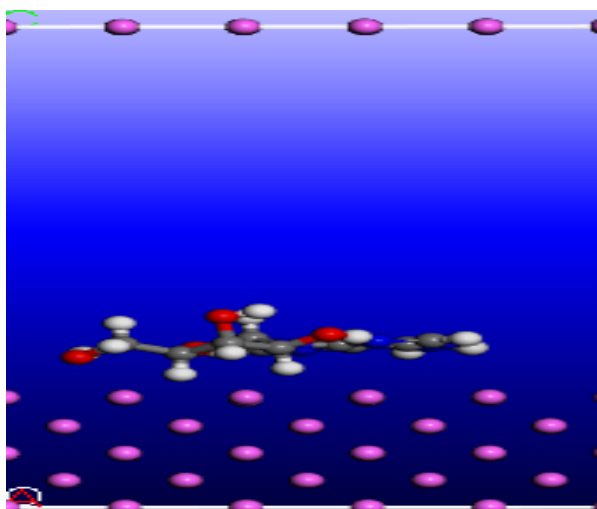


Figure 1. Mode of adsorption of VDB on the surface of the aluminum

Table 1. The energy of the interaction between Al(110) and VDB

Properties VDB	Al (kJ.mol^{-1})
Total Potential Energy	-9.722 ± 0.1
Energy of the Molecule	49.200 ± 0.0
Total kinetic energy	16.884 ± 2.2
Energy of Al (110)	0.000 ± 0.0
Adsorption energy	-58.923 ± 0.1
Binding energy	58.923 ± 0.1

Frontier Molecular Orbitals

When the bond lengths of the compound were compared before and after simulation, the molecules with double bonds were shorter, demonstrating that high energy is required for such a bond to break down, while the molecules with single bonds were longer, demonstrating

that such bonds did not require much energy for the breakdown [1,2]. Figure 3 depicts that the molecule interacted with the aluminum surface and that electrons had undoubtedly been transferred between the surface and the molecule [4]. The bond locations N10-C11, C1-N2, N2=C3, C14-C12, O12-C13, C13-C16, C16-O17, and C11-C15 all exhibit a noticeable change

in bond length, showing that the molecule has surface contact with the metal [25,32,33]. Both versions of all the examined molecules are entirely planar, as evidenced by the torsional angles in Table 2 of optimized structures and the simulated structure values [27]. This is also shown in the horizontal orientation of the molecule encounter with the surface as depicted

in Figure 1. This demonstrates that molecules tend to adsorb to metal surfaces in a flat orientation, maximizing the surface coverage [10]. Salient bond lengths in the molecules were compared between the simulated and optimized versions to explain the molecule's impact on the surface during interaction [27].

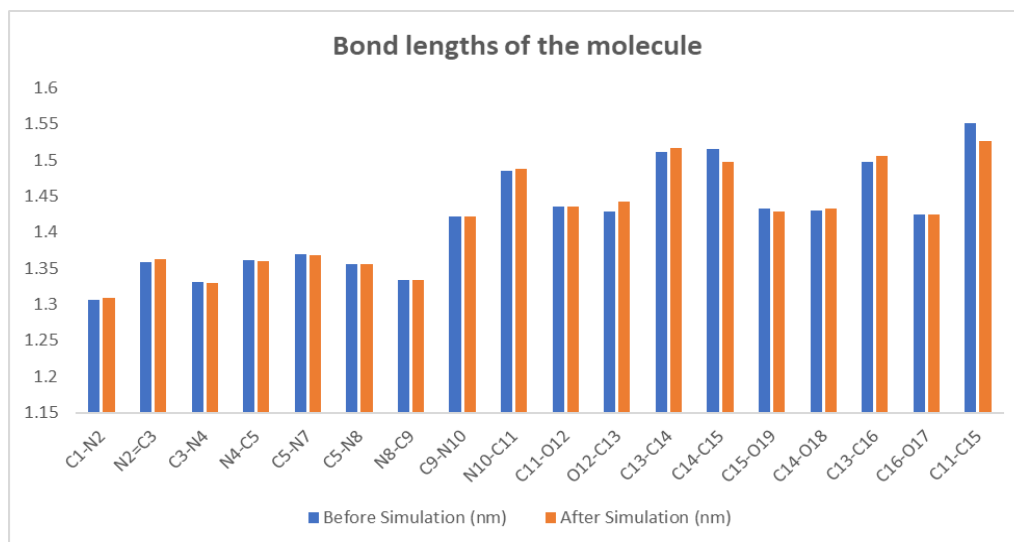


Figure 2. Calculated link length (\AA) of the molecule VDB before and after simulation

Table 2. Rotational constants of H_2 , DH, and D_2

Torsion Atoms	Before simulation (φ°)	After stimulation (φ°)
C1-N2=C3-N4	-0.562	1.245
N4-C5-C6-N8	179.932	178.785
N8-C6-C5-N7	-0.512	1.328
N8-C9-N10-C11	166.177	163.463
C9-N10-C11-O12	28.974	35.472
O12-C13-C16-O17	63.178	66.208
O17-C16-C13-C14	77.826	169.304
O19-C15-C14-O18	16.744	48.616

Active site

Molecules' local reactivity improves efficiently during electron transfer by picking where the reaction is most likely to occur, either by providing or absorbing electrons [4,5]. The radical Fukui function (f^0), electrophilic Fukui function (f), and nucleophilic Fukui function (f^+)

all reveal a molecule's point of attack [10,15,19]. The only Fukui functions studied in this work were the nucleophilic (f^+) and electrophilic (f). The findings of those with the most significant values are displayed in Figure 3 [4]. Figure 4 demonstrates the results of the Fukui second function, which computes the nucleophilic and electrophilic nature of the molecule.

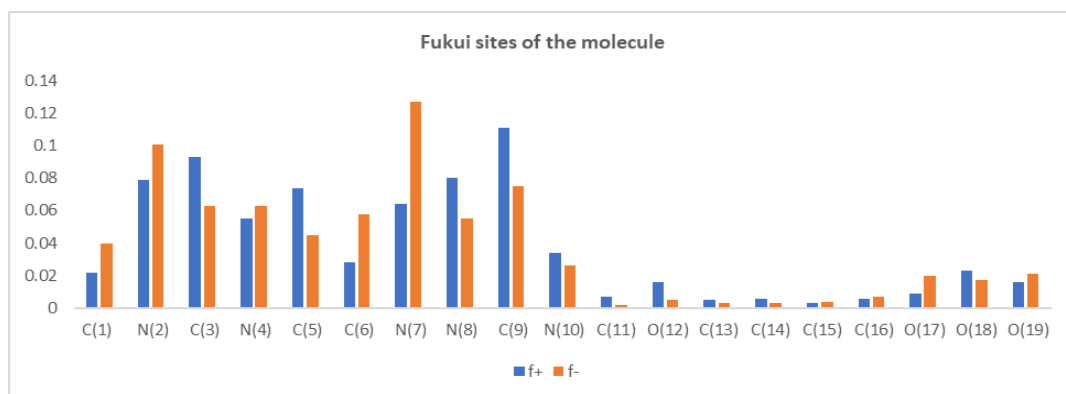


Figure 3. The Fukui functions of the Molecule VDB

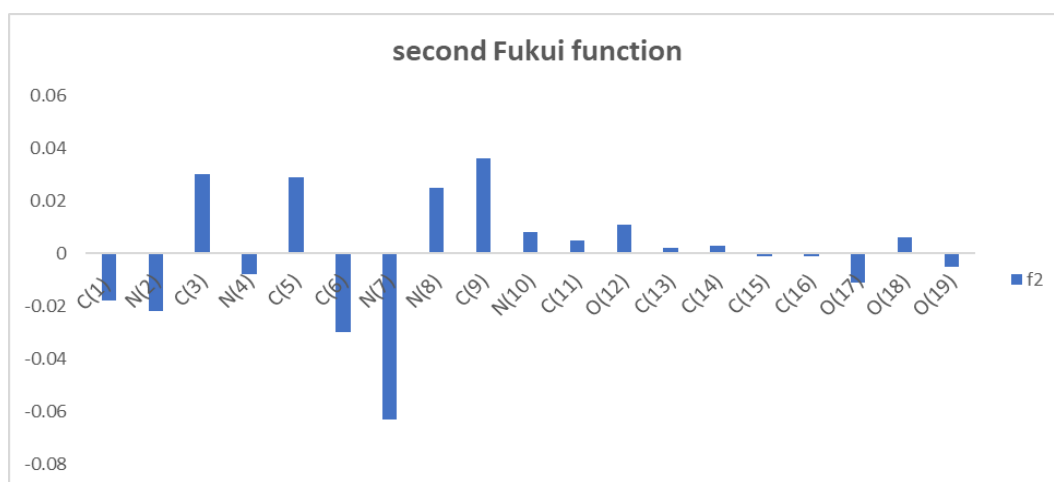


Figure 4. The calculated Fukui function of the molecule

According to Figure 3, N7 had the highest F-function for electron transport per atom, while N2 had the highest F^+ function. This suggests that electrons are transferred to the metallic surface at position N2 and that the molecule gains extra electrons at position N7 [29,30]. The second Fukui function in Figure 4 shows that the molecule is nucleophilic, meaning that it transfers electrons to aluminum's p -orbital faster than it returns them to the inhibitor from the p -orbitals [20].

Quantum Chemical Parameters

Figure 5 demonstrated the Optimized molecule, HOMO orbitals, Electron Density and LUMO orbitals of the molecule under study. Through

the HOMO and the LUMO orbitals, the quantum chemical parameters were obtained through equations 1-12 as presented in Table 3.

Ionization energy is the amount of energy a molecule requires to liberate one electron from the surface of an atom when it is in a gaseous state, while electron affinity is the measure of an atom's ability to absorb an electron [10]. In other words, an examination of the ionization potential (IE) and electron affinity (EA) may be used to anticipate the amount of energy that is released by a molecule during the inhibitor-metal adsorption process when an electron is lost and gained [20,34]. Both the measurements for the electron affinity and the ionization potential for the VDB molecule under study were in good agreement. According to the estimated quantum

parameters results, the molecule VDB has a half-electron transfer value of less than 3.6. According to the literature, if ΔN is less than 3.6, the effectiveness of the inhibition increases as the molecules' ability to donate electrons rises.

However, if ΔN is greater, the effectiveness of the inhibition decreases as the inhibitor's ability to donate electrons rises [1,10,21]. The formal scenario for the structure under study is one with a VDB molecule on an aluminum surface.

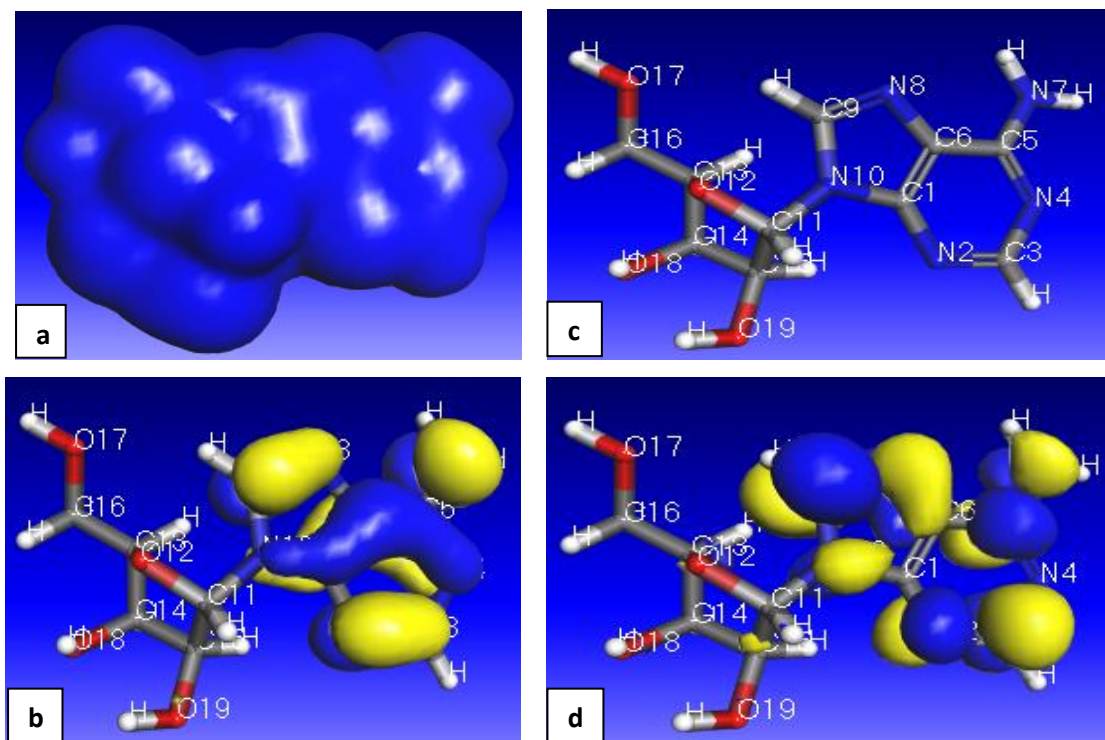


Figure 5. (a) Optimized molecule (b) HOMO orbitals (c) Electron Density (d) LUMO orbital

Table 3. Energy parameters of the molecule VDB

Parameters studied	VDB
E_{HOMO} (eV)	-5.050
E_{LUMO} (eV)	-1.158
IP (eV)	5.050
EA (eV)	1.158
ΔE (eV)	3.892
electronegativity(χ)	3.104
Global hardness (η)	1.946
Global softness(S)	0.514
Global electrophilicity index	2.476
Nucleophilicity	0.404
Half-electron transfer(ΔN) Al	0.641
(ω^-) Electron donating power	4.271
(ω^+) Electron accepting power	1.167
(ΔE_{bd}) Back donation	-0.487

A lower value of ELUMO produces a higher electron-acceptance capacity of molecules from the surface of aluminum. The ability of the inhibitor to assign electrons to the open d-orbital on the metal surface improves the efficiency of the inhibition process [1,2]. The fact that E_{HOMO} values are negative suggests that physical adsorption is preferred when molecules and metals are adsorbed to their surfaces [1,9,15,18]. Additionally, molecules with higher E_{HOMO} values have a higher propensity to transfer electrons to the surface of aluminum. The E_{LUMO} and E_{HOMO} levels must differ for the molecule's stability indicator to function correctly. A compound with a low energy gap (ΔE_{g}) has higher inhibition efficiency, which lowers the excitation energy required to remove an electron from the last occupied orbital [1,10]. In its most basic form, chemical hardness refers to resistance to polarization or distortion of the electron cloud of atoms, ions, and molecules in the presence of minute chemical reaction disturbances. In contrast to the large energy gap of a hard molecule, soft molecules have a smaller energy gap. The molecule's energy gap can be used to determine its softness [16,17,28].

The back donation Eb-d energy was also used to discuss the contact effect between the inhibitor VDB and the aluminum surface. If the global hardness is positive and the energy of back donation (Eb-d) value is negative, the back donation process is favored so that the molecule transmits the charge to the aluminum metal when they come in contact with the surface of the Al. In contrast, the electrophilicity index indicates a molecule's ability to accept electrons (ω). The ability of a molecule to provide or receive electrons is referred to as nucleophilicity (ϵ), which is the opposite of electrophilicity ($1/\omega$). According to research, compounds with high nucleophilicity values successfully prevent corrosion compared to molecules with high electrophilicity indices. This finding was in line with a study on a related compound by Iorhuna

et al. and Nyijime et al. [18,20]. The power of the electron donator and acceptor estimated from the molecule obtained from the computation was high, indicating that the molecule has a greater capacity to donate an electron to the aluminum surface, as previously demonstrated by the Second Fukui function in a system's ability to accept charge is strengthened by a higher electron accepting power (ω^+) value. In contrast, a lower electron-donating power (ω^-) value improves its ability to donate charge [7].

Conclusion

As determined by the values of interaction/binding energy, bond length, and quantum chemical parameters such as the energy of the highest occupied molecular orbital (EHOMO), the energy of the lowest unoccupied molecular orbital (ELUMO), energy gap (E), total energy (E), electron affinity (A), ionization potential (I), and others, from the result it can be concluded that: (a) The inhibition process was driven by the transfer of electrons between the metal crystal surface and the molecule, as shown by the number of electron transfer (ΔN) values for the surface; (b) According to a molecular dynamic simulation, the adsorption happened by a process called physisorption, which accounts for the low value of binding energy between the surface and the molecule; (c) Molecular Dynamic (MD) and Density Functional Theory (DFT) simulations may be particularly effective techniques for rationalizing various potential corrosion inhibitors; (d) *Vidarabine* is a suitable corrosion inhibitor for aluminum metal.

Acknowledgment


The authors wish to acknowledge the contribution of Dr. A. M. Ayuba of Pure and Industrial Chemistry Bayero University, Kano, Nigeria. for the success of this research.

Disclosure statement

The authors declare that they have no conflict of interest

Orcid

Fater Iorhuna : [0000-0002-1018-198X](https://orcid.org/0000-0002-1018-198X)

Abdullahi Muhammad Ayuba : [0000-0002-2295-8282](https://orcid.org/0000-0002-2295-8282)

Thomas Aondofa Nyijime : [0000-0001-9537-1987](https://orcid.org/0000-0001-9537-1987)

Muhammad Shuaibu : [0009-0006-3684-5461](https://orcid.org/0009-0006-3684-5461)

References

- [1] T. Nagalakshmi, A. Sivasakthi. *Int. J. Innov. Technol. Explor. Eng.*, **2019**, *9*, 1568–1572. [[CrossRef](#)], [[Google Scholar](#)], [[Publisher](#)]
- [2] A.O. Okewale, Adebayo A.T. *Niger. J. Technol.*, **2020**, *39*, 173–181. [[CrossRef](#)], [[Google Scholar](#)], [[Publisher](#)]
- [3] H.A. Al Mashhadani, K.A. Saleh, *Iraq. J. Sci.*, **2020**, *61*, 2751–2761. [[CrossRef](#)], [[Google Scholar](#)], [[Publisher](#)]
- [4] L. Afandiyeva, V. Abbasov, L. Aliyeva, S. Ahmadbayova, E. Azizbeyli, HM. El-Lateef Ahmed, *Iran. J. Chem. Chem. Eng.*, **2018**, *37*, 73-79. [[CrossRef](#)], [[Google Scholar](#)], [[Publisher](#)]
- [5] H. Jafari, F. Mohsenifar, K. Sayin, *Iran. J. Chem. Chem. Eng.*, **2018**, *37*, 85–103. [[CrossRef](#)], [[Google Scholar](#)], [[Publisher](#)]
- [6] S. Elmi, MM. Foroughi, M. Dehdab, M. Shahidi-Zandi, *Iran. J. Chem. Chem. Eng.*, **2019**, *38*, 185–200. [[CrossRef](#)], [[Google Scholar](#)], [[Publisher](#)]
- [7] B.N. Noorollahy, H.R. Hafizi-Atabak, F. Atabaki, M. Radvar, S. Jahangiri, *Iran. J. Chem. Chem. Eng.*, **2020**, *39*, 113–25. [[CrossRef](#)], [[Google Scholar](#)], [[Publisher](#)]
- [8] L.T. Popoola, T.A. Aderibigbe, M.A. Lala, *Iran. J. Chem. Chem. Eng.*, **2022**, *41*, 482–492. [[CrossRef](#)], [[Google Scholar](#)], [[Publisher](#)]
- [9] R.M. Kubba, N.M. Al-Joborry, *Iraq. J. Sci.*, **2021**, *62*, 1396–1403. [[CrossRef](#)], [[Google Scholar](#)], [[Publisher](#)]
- [10] K.A.K. Al-Rudaini, K.A.S. Al-Saadie, *Iraq. J. Sci.*, **2021**, *62*, 363–372. [[CrossRef](#)], [[Google Scholar](#)], [[Publisher](#)]
- [11] M.A. Mohammed, R.M. Kubba, *Iraq. J. Sci.*, **2020**, *61*, 1861–1873. [[CrossRef](#)], [[Google Scholar](#)], [[Publisher](#)]
- [12] S. Mammeri, N. Chafai, H. Harkat, R. Kerkour, S. Chafaa, *Iran. J. Sci. Technol. Trans. Sci.*, **2021**, *45*, 1607–1619. [[CrossRef](#)], [[Google Scholar](#)], [[Publisher](#)]
- [13] T.V. Kumar, J. Makangara, C. Laxmikanth, N.S. Babu, *Int. J. Comput. Theor. Chem.*, **2016**, *4*, 1–6. [[CrossRef](#)], [[Google Scholar](#)], [[Publisher](#)]
- [14] T.O. Esan, O.E. Oyeneyin, A. Deola, N.I. Olanipekun, *Adv. J. Chem. A*, **2022**, *5*, 263–270. [[CrossRef](#)], [[Google Scholar](#)], [[Publisher](#)]
- [15] R.M. Kubba, N.M. Al-Joborry, N.J. Al-lami, *Iraq. J. Sci.*, **2020**, *61*, 2776–2796. [[CrossRef](#)], [[Google Scholar](#)], [[Publisher](#)]
- [16] Z. Yavari, M. Darijani, M. Dehdab, *Iran. J. Sci. Technol. Trans. Sci.*, **2018**, *42*, 1957–1967. [[CrossRef](#)], [[Google Scholar](#)], [[Publisher](#)]
- [17] N.M. Al-Joborry, R.M. Kubba, *Iraq. J. Sci.*, **2020**, *61*, 1842–1860. [[CrossRef](#)], [[Google Scholar](#)], [[Publisher](#)]
- [18] F. Iorhuna, A. M. Ayuba, N. A. Thomas, *Mor. J. Chem.*, **2023**, *11*, 884–896. [[CrossRef](#)], [[Google Scholar](#)], [[Publisher](#)]
- [19] M.E. Belghiti, S. Echihi, A. Dafali, Y. Karzazi, M. Bakasse, H. Elalaoui-Elabdallaoui, L.O. Olasunkanmi, E.E. Ebenso, M. Tabyaoui, *Appl. Surf. Sci.*, **2019**, *491*, 707–722. [[CrossRef](#)], [[Google Scholar](#)], [[Publisher](#)]
- [20] T.A. Nyijime, H.F. Chahul A.M. Ayuba. F. Iorhuna, *Adv. J. Chem. A*, **2023**, *6*, 141–154. [[CrossRef](#)], [[Google Scholar](#)], [[Publisher](#)]
- [21] M.M. Kadhim, L.A.A. Juber, A.S.M. Al-Janabi, *Iraq. J. Sci.*, **2021**, *62*, 3323–3335. [[CrossRef](#)], [[Google Scholar](#)], [[Publisher](#)]

- [22] D. Glossman-Mitnik, *Procedia Comput. Sci.*, **2013**, *18*, 816–825. [[CrossRef](#)], [[Google Scholar](#)], [[Publisher](#)]
- [23] A. Nahlé, R. Salim, F. El Hajjaji, MR. Aouad, M. Messali, E. Ech-Chihbi, B. Hammouti, M. Taleb, *RSC Adv.*, 2021, *11*, 4147–4162. [[CrossRef](#)], [[Google Scholar](#)], [[Publisher](#)]
- [24] N.O. Eddy, P.O. Ameh, N.B. Essien, *J. Taibah Univ. Sci.*, **2018**, *12*, 545–56. [[CrossRef](#)], [[Google Scholar](#)], [[Publisher](#)]
- [25] L. Guo, M. Zhu, J. Chang, R. Thomas, R. Zhang, P. Wang, X. Zheng, Y. Lin, R. Marzouki, *Int. J. Electrochem. Sci.*, **2021**, *16*, 211139. [[CrossRef](#)], [[Google Scholar](#)], [[Publisher](#)]
- [26] H. Lgaz, S. Masroor, M. Chafiq, M. Damej, A. Brahmia, R. Salghi, M. Benmessaoud, I.H. Ali, M.M. Alghamdi, A. Chaouiki, I.M. Chung, *Metals*, **2020**, *10*, 357. [[CrossRef](#)], [[Google Scholar](#)], [[Publisher](#)]
- [27] F. Iorhuna, N.A. Thomas, S.M Lawal, *Alger. J. Eng. Technol.* **2023**, *8*, 43–51. [[Google Scholar](#)], [[Publisher](#)]
- [28] G. Kılınççeker, M. Baş, F. Zarifi, K. Sayın, *Iran. J. Sci. Technol. Trans. Sci.*, **2021**, *45*, 515–527. [[CrossRef](#)], [[Google Scholar](#)], [[Publisher](#)]
- [29] O.O Emmanuel, O.B. Samuel, O.F. Kolawole, A.D. Dada, A.E. Oluwafisayo, E.B. Chibuzo, I. Nureni, *Adv. J. Chem. B*, **2020**, *2*, 197–208 [[CrossRef](#)], [[Google Scholar](#)], [[Publisher](#)]
- [30] F. Iorhuna, A.S. Muhammad, A.M. Ayuba. *Adv. J. Chem. A*, **2023**, *6*, 71–84. [[CrossRef](#)], [[Google Scholar](#)], [[Publisher](#)]
- [31] A.U. Bello, A. Uzairu, G.A. Shallangwa. *Port. Electrochim. Acta*, **2020**, *38*, 377–386. [[Google Scholar](#)]
- [32] A. Vojood, M.M. Khodadadi., R.G., Ebrahimzadeh S. Mohajeri, A. Shamel. *Iran. J. Chem. Chem. Engin.*, **2022**, *41*, 3333–3340. [[CrossRef](#)], [[Google Scholar](#)], [[Publisher](#)]
- [33] M.M. Alizadeh, F. Salimi. G.E. Rajaei, *Braz. J. Phys.*, **2022**, *52*, 56. [[CrossRef](#)], [[Google Scholar](#)], [[Publisher](#)]
- [34] R. Razavi., S.M. Abrishamifar, G.E Rajaei, M.R.R. Kahkha, M. Najafi, *J. Mol. Model.*, **2018**, *24*, 64. [[CrossRef](#)], [[Google Scholar](#)], [[Publisher](#)]

HOW TO CITE THIS ARTICLE

Fater Iorhuna*, Ayuba Abdullahi Muhammad, Thomas Aondofa Nyijime, Muhammad Shuaibu. A DFT and Molecular Dynamic (MD) Simulation on the Adsorption of Vidarabine as a Potential Inhibitor on the Al Metal surface, *Adv. J. Chem. A*, 2023, 6(4), 380-390.

DOI: [10.48309/AJCA.2023.409740.1390](https://doi.org/10.48309/AJCA.2023.409740.1390)

URL: https://www.ajchem-a.com/article_178007.html